Compton **scattered** radiation imaging and Bimodality

Mai K. Nguyen

ETIS-CNRS 8051 / ENSEA/ Université de Cergy-Pontoise, France

mai.nguyen-verger@u-cergy.fr

Interdisciplinary Symposium on Signals and Systems for Medical Applications
3-4 June 2013 Paris France

Contents

1) Principle of Compton Scattered Radiation Imaging

PRINCIPLE:
The necessary information for reconstruction does not come from **primary** transmitted rays but from **deflected** rays by Compton scattering

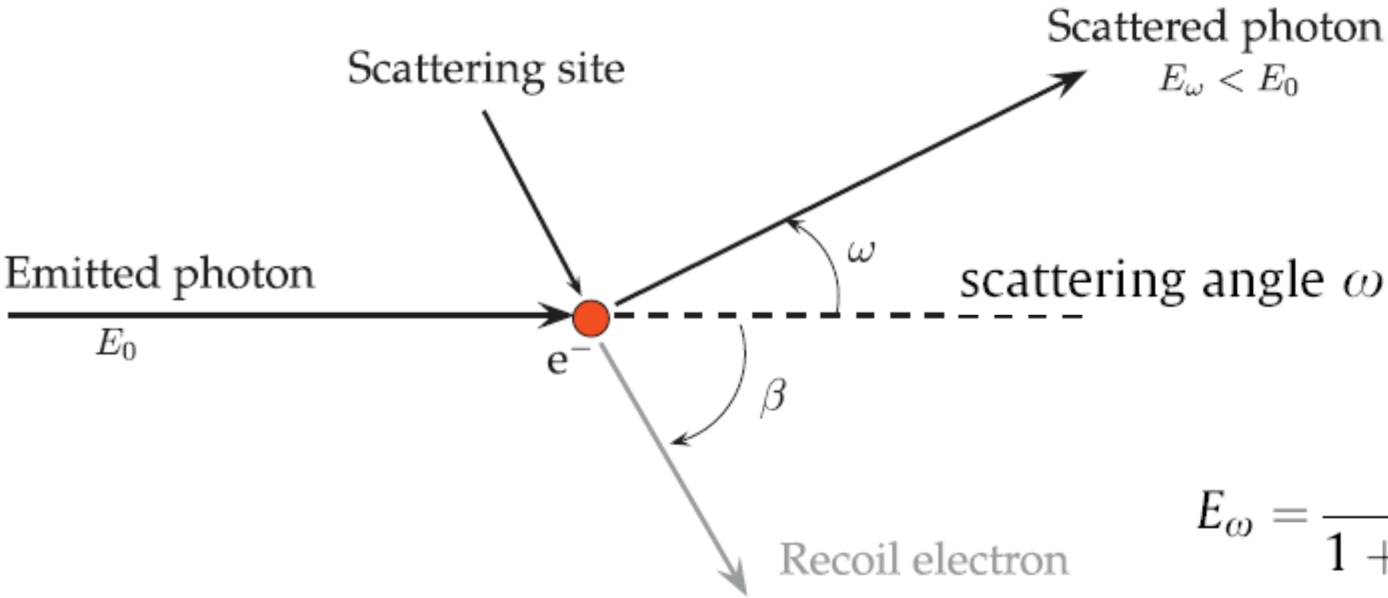

$$E_\omega = \frac{E_0}{1 + \frac{E_0}{mc^2}(1 - \cos\omega)}$$

Compton scattering of radiation (photons) by electrons

Principle of Scattered Radiation Imaging

❖ What is measured is the number of scattered photons of given energy E_ω at a given pixel site.

❖This number is due to the contributions of many source sites (or scattering sites when the source is fixed) lying on surfaces in 3D and curves in 2D.

❖ As the detection pixel varies in space, the measurement process is modelled by generalized Radon transforms, which are integrals of activity density (or electron density) on surfaces (or curves).

❑ In scattered radiation emission imaging, the electron density is assumed to be known, the unknown quantity is the activity density.

❑ In transmission – scattering imaging, the external source is known and the unknown is the object electron density.

❖ Solving for the unknown density is an inverse problem, which requires

the **inversion** of **generalized Radon transforms**

2) Compton scattered radiation imaging modalities

A) Emission Imaging

(Radiating objects with source activity distribution):

- 3 D imaging (2002)
- 2 D imaging (2010)

B) Transmission Imaging

In two dimensions called Compton scattering Tomography (CST)

(Objects subjected to fixed external radiation source):

- S J Norton's modality (1995)
- A new modality (2010)

C) Bimodality:

A combination of emission and transmission scattering modalities

A review of conventional Emission Imaging: SPECT

- ❑ Data: Linear projections of activity density at energy E_0
- ❑ Modeling by X-ray transform of activity density along straight lines along all possible directions
- ❑ Reconstruction of activity by inversion of X-ray transform (existing)

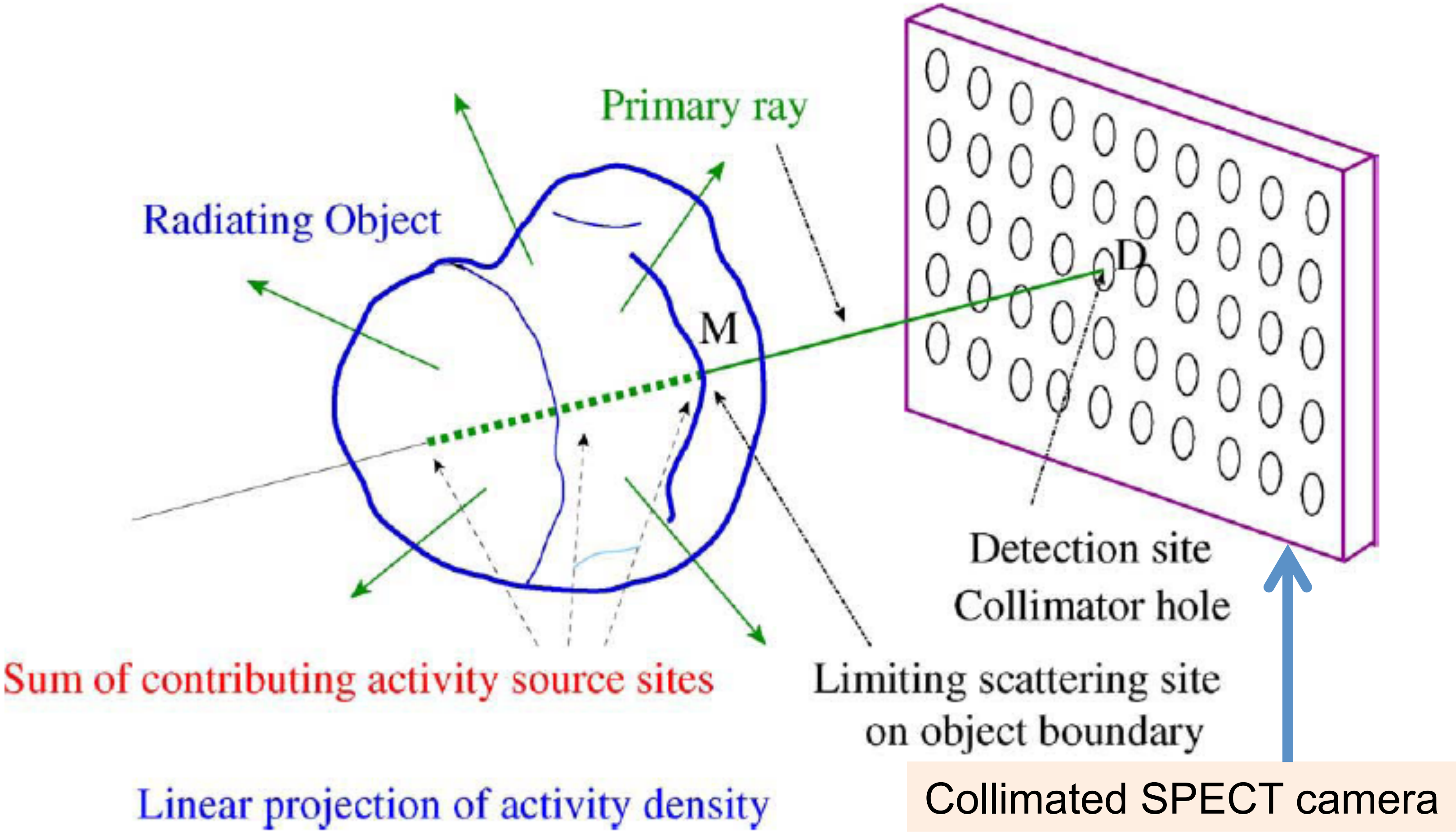

Scattered Radiation SPECT imaging

- **Concept of compounded conical projection** of activity density at energy $E < E_0$
- **Compounded conical Radon transform** (CCRT) for all scattering angles (or energy E) and all detection sites D, electron density assumed known

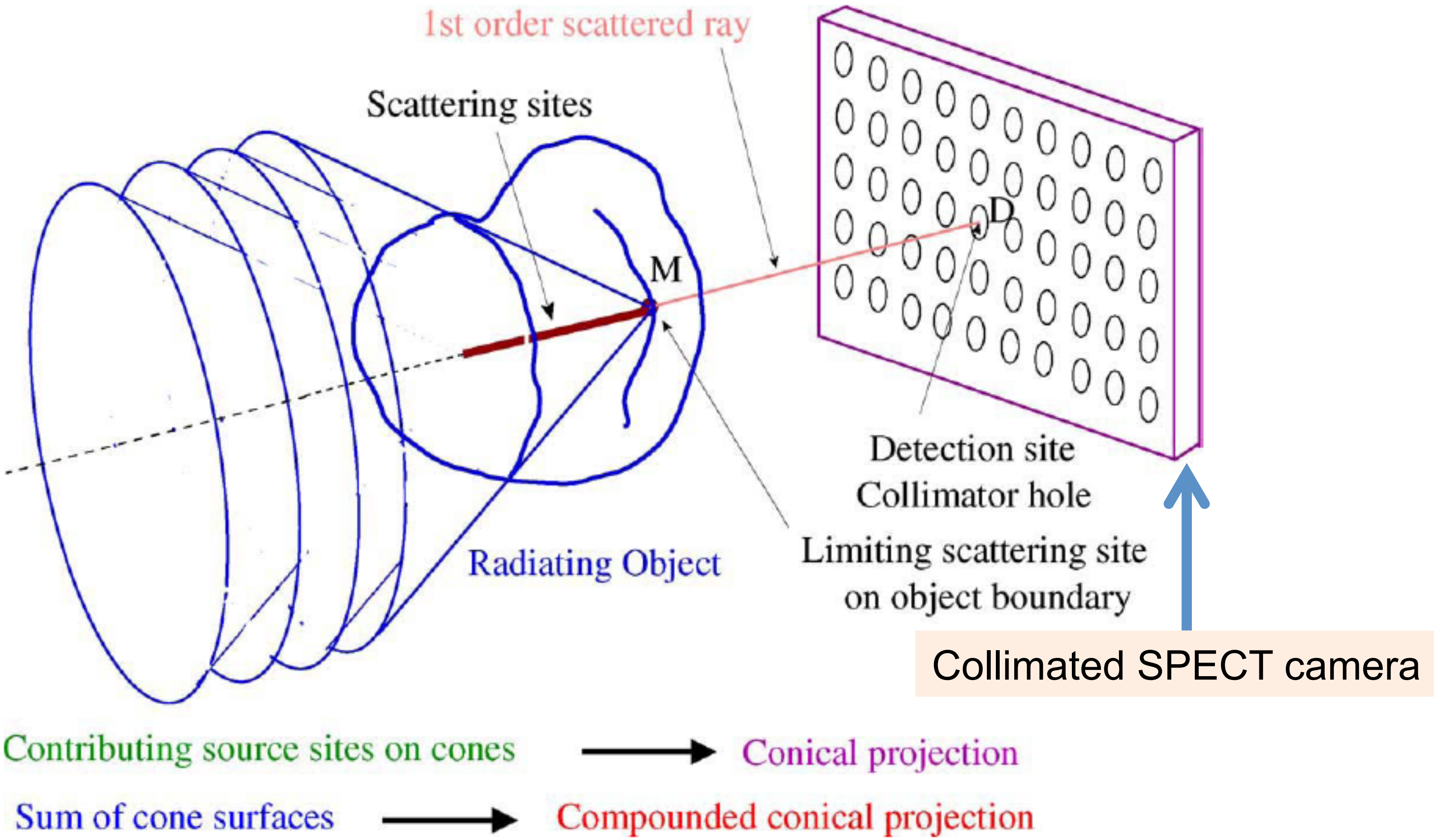

Linear versus Conical projections

Conventional detection of **primary** radiation by a collimated gamma camera

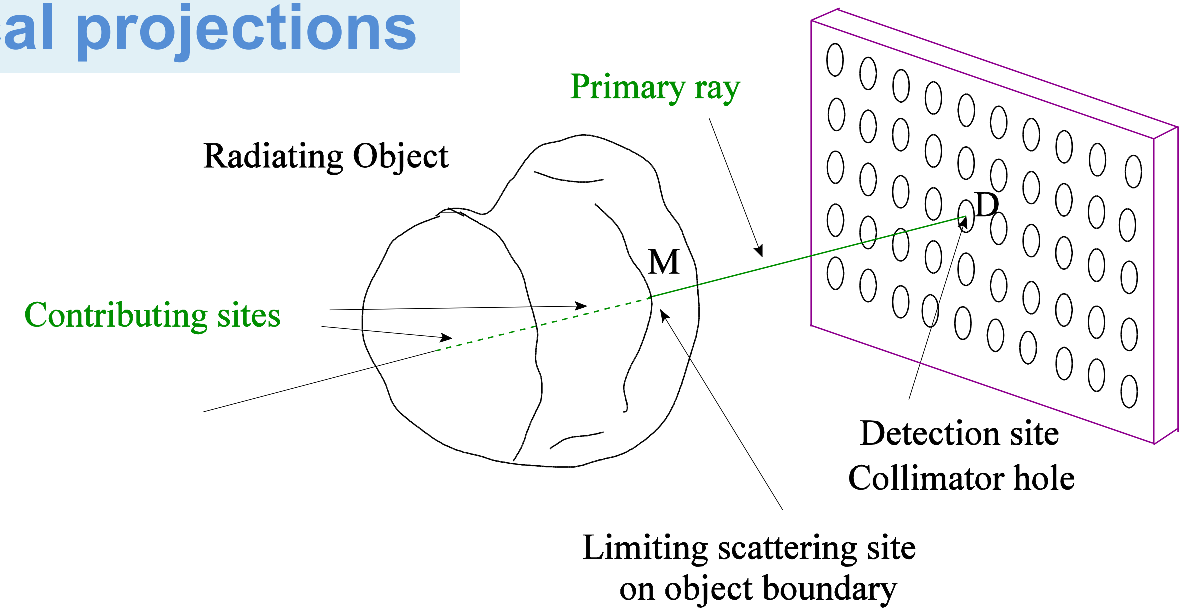

Detection of first order **scattered** radiation by gamma camera

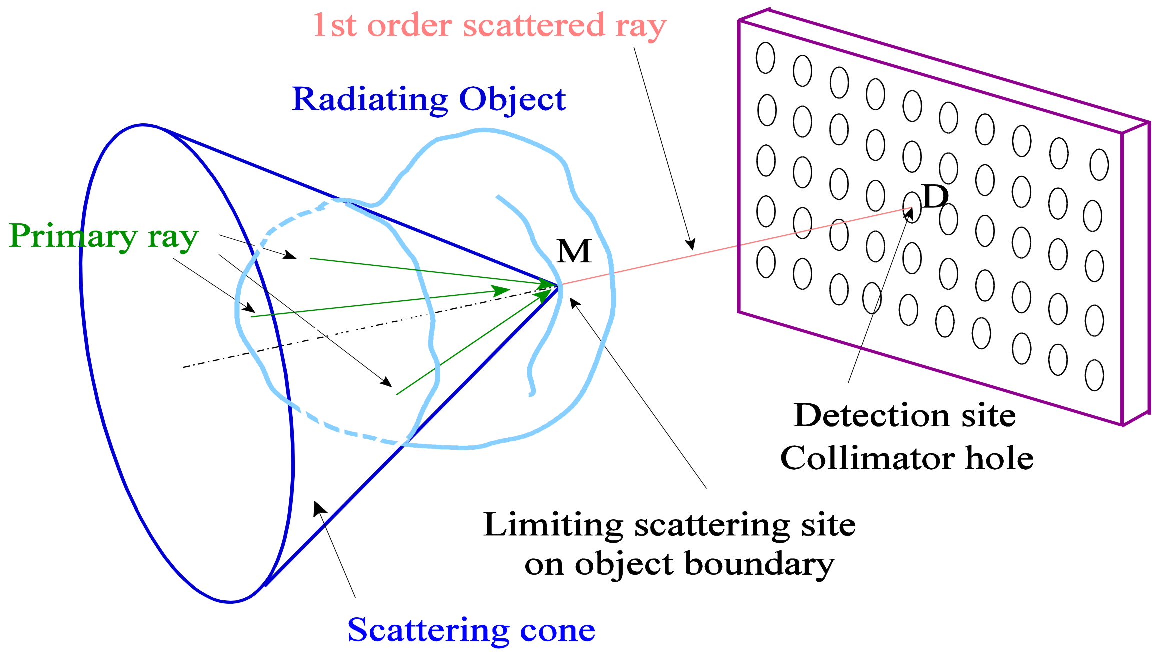

Analysis of the photon detection on SPECT camera

Detection of scattered radiation by collimated gamma camera

Contributions of scattered radiation at one detection site

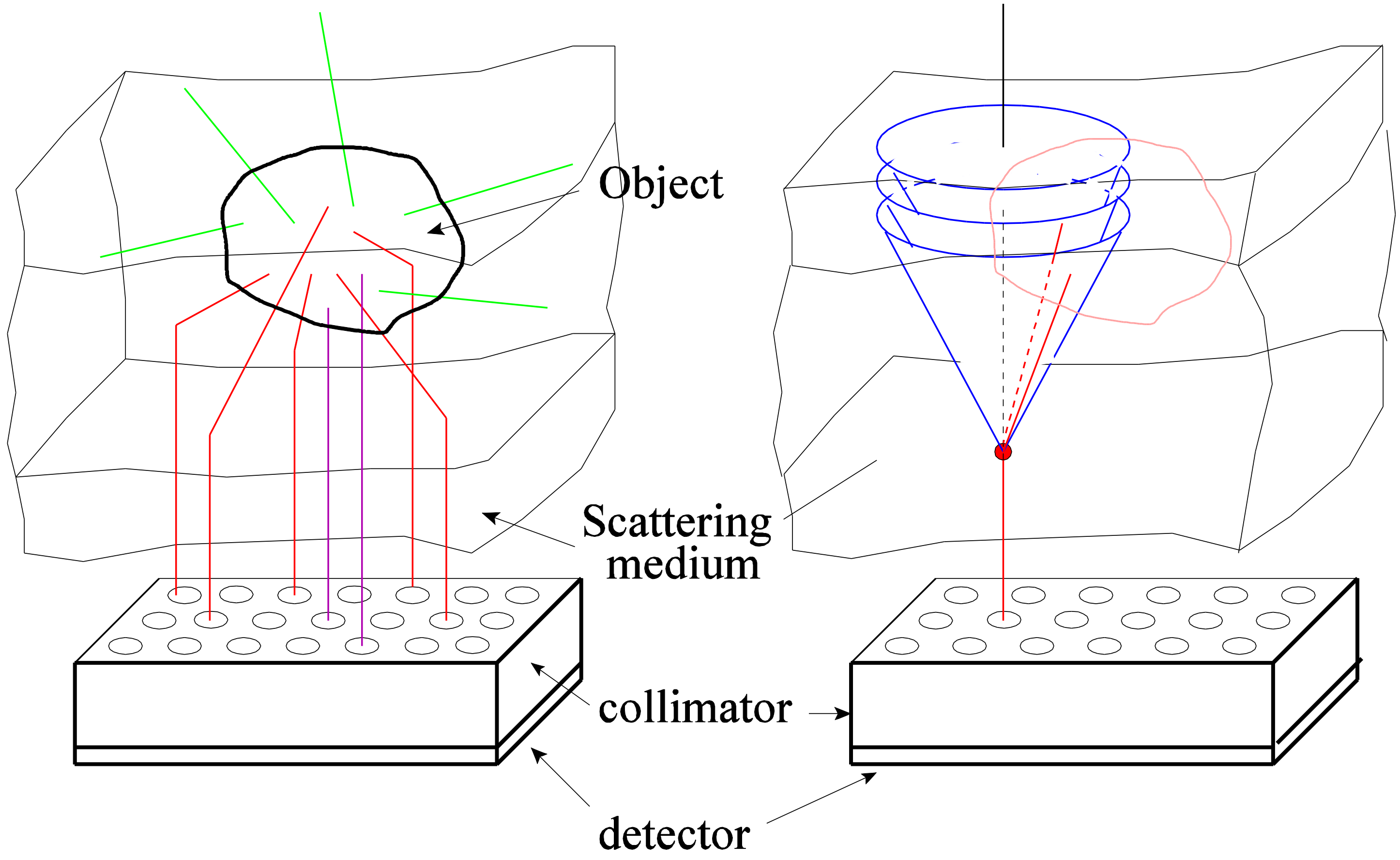

Scattered Radiation Emission Imaging

❑ Object is characterized by activity density (radiating object)
❑ Detection pixel on collimated SPECT type γ-camera
❑ Flux density of detected scattered photons at site D is due to
- all the scattering sites M on a line perpendicular to the γ-camera plane
- all emission sites S on circular cones of apex opening angle ω and the locus of all scattering sites as symmetry axis

➢For given electron density, the detected photon flux density at a site of the γ-camera is given by
- an integral of the activity density over the surface of a circular cone and
- an integral over the line of scattering sites

➢Such an integral, which represents the scattered radiation emission data is a function of three variables: the two coordinates of site D on the γ-camera and the photon scattered energy E (or the scattering angle ω).

➢In two dimensions, the data is function of two variables: the abscissa of the detecting site on a linear γ-camera and ω the scattering angle.

Image formation modelling by the Compounded Conical Radon transform of

object activity density $f(x, y, z)$

$$\widehat{f}(x_D, y_D, \omega) = \int_{\mathbb{R}^3} dx\, dy\, dz\, \mathcal{K}_{PSF}(x_D, y_D, \omega | x, y, z)\, \overline{f}(x, y, z)$$

where

$$\overline{f}(x, y, z) = \int_0^\infty d\zeta\, \nu(\zeta)\, f(x, y, z + \zeta)$$

integration kernel

$$\mathcal{K}_{PSF}(x_D, y_D, \omega | x, y, z)$$

$$= K(\omega)\ \nu(\sqrt{(x - x_D)^2 + (y - y_D)^2 + (z - \zeta)^2})$$

$$\times\ \delta(\cos\omega \sqrt{(x - x_D)^2 + (y - y_D)^2} - (z - \zeta) \sin\omega)$$

$K(\omega)$ is the Compton kinematic factor

$\nu(d)\ =\ 1/d^2$ (photometric factor)

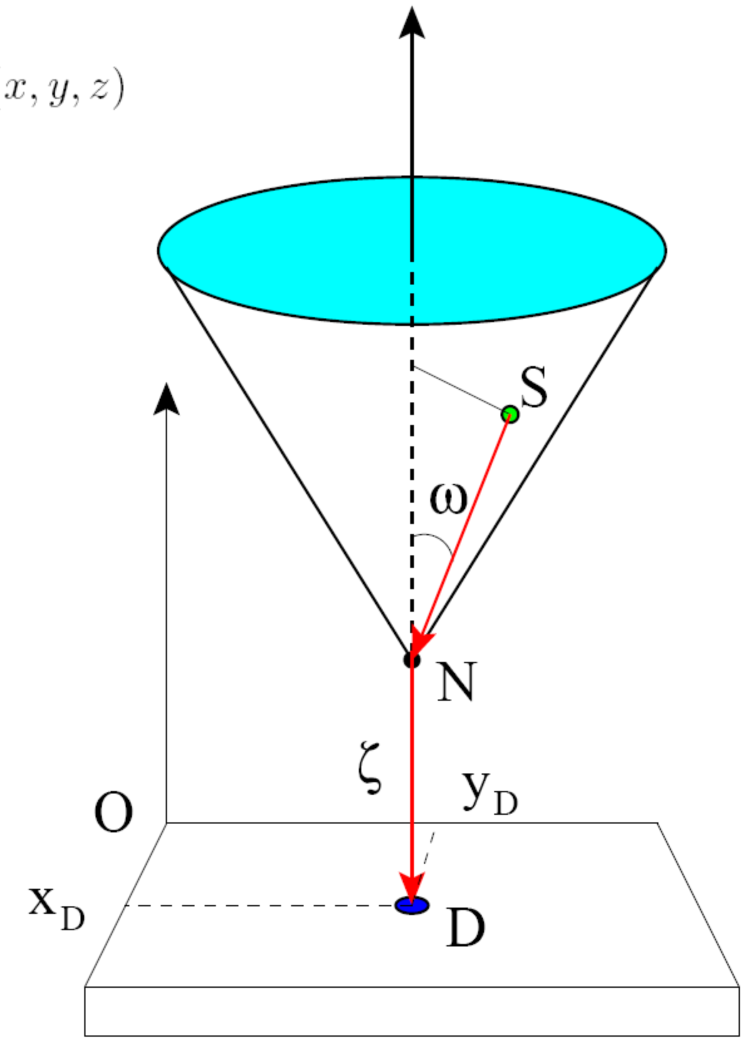

Reconstruction of activity by inversion of the Compounded Conical Radon Transform

The Fourier transform of $f(x, y, z)$ verifies

$$\widetilde{f}(u, v, w) = \int_{\mathbb{R}} d\sigma \exp[2i\pi\sigma w] \frac{[-|z|\sqrt{u^2+v^2}]}{\mathcal{J}(w)} \int_{\mathbb{R}_+} t\, dt\, J_1(2\pi|z|t\sqrt{u^2+v^2})$$

$$\left[H(\omega - \pi/2)\frac{\partial}{\partial t}\frac{G(u, v, t)}{K(t)} + H(\pi/2 - \omega)\frac{\partial}{\partial t}\frac{G(u, v, -t)}{K(-t)}\right],$$

where

- $\mathcal{J}(w)$ is the Fourier transform of $\nu(x)$,
- $J_1(x)$ is the Bessel function of order 1,
- $H(x)$ is the Heaviside unit step function,
- $t = \tan\omega$,
- $G(u, v, t)$, the Fourier transform of $\widehat{f}(x_D, y_D, \omega)$

$f(x, y, z)$ is recovered by three-dimensional inverse Fourier transform

Hence discarding attenuation, under the following conditions:

- first order scattering events are accounted for since they are vastly dominant and higher order scattering are neglected ,
- the electron density is assumed to be constant. This is a reasonable hypothesis since most human tissues (brain cells, blood, muscles, lung tissues, water, etc) have an electron density around 3.4×10^{23} cm^{-3}. Their density is also around 1.0g.cm^{-3} This means for our purpose, objects containing bones should not be considered,
- the set of compounded conical projections has one fixed direction $\mathbf{n}$, parallel to the Oz axis direction,
- the set of detecting pixels are distributed as array on a two-dimensional area, forming a collimated SPECT gamma camera.

❑ Reconstruction is analytically possible
❑ Data is collected by non-rotating Gamma camera

One may say that the usual spatial rotation angle is replaced by the scattering angle in this modality

Realistic working factors (attenuation, noise, radiation spreading, etc.) may be taken into account in later steps

3D Reconstruction results

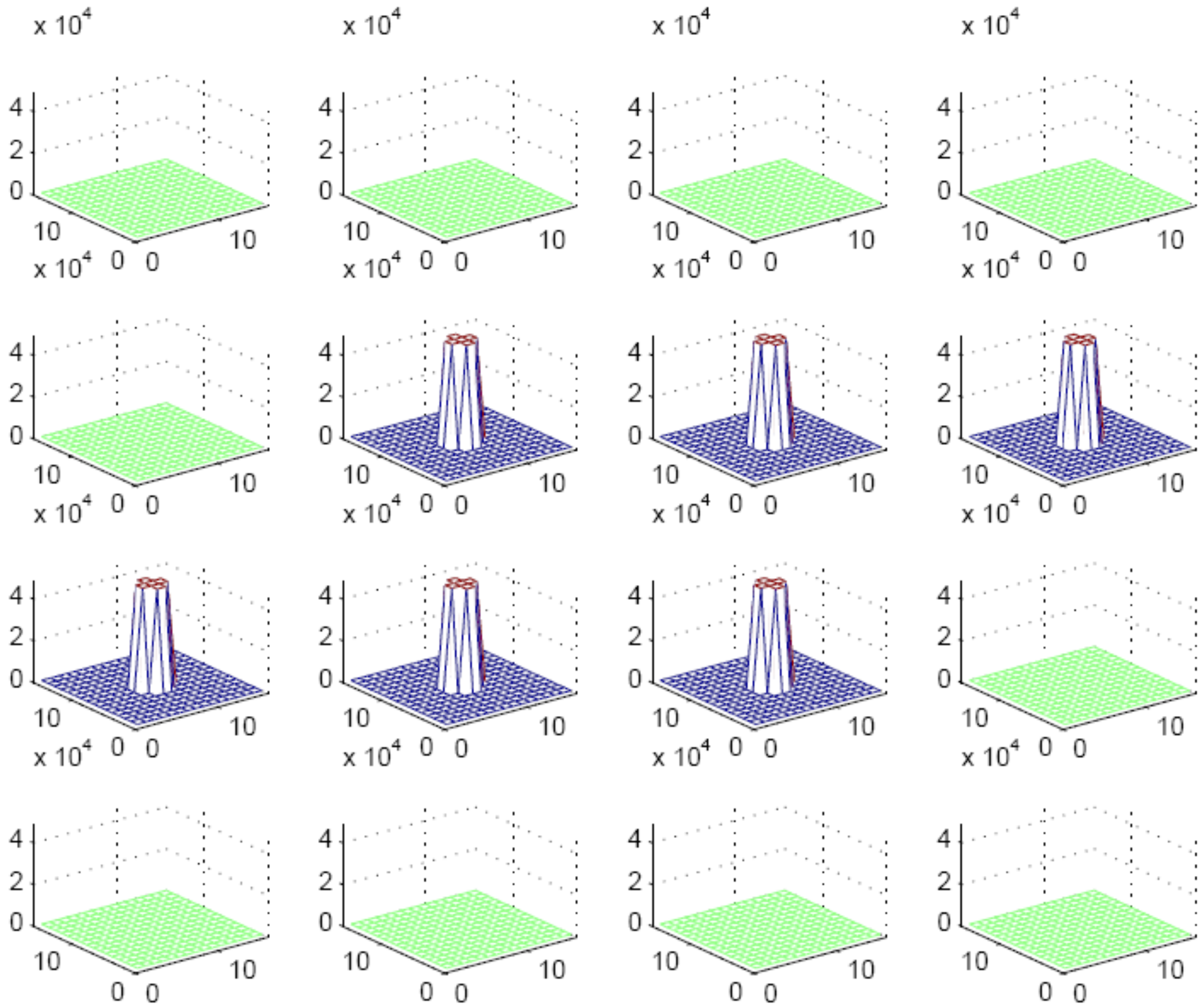

Original object (cylinder) in a cube consisting of 16 transaxial planes.

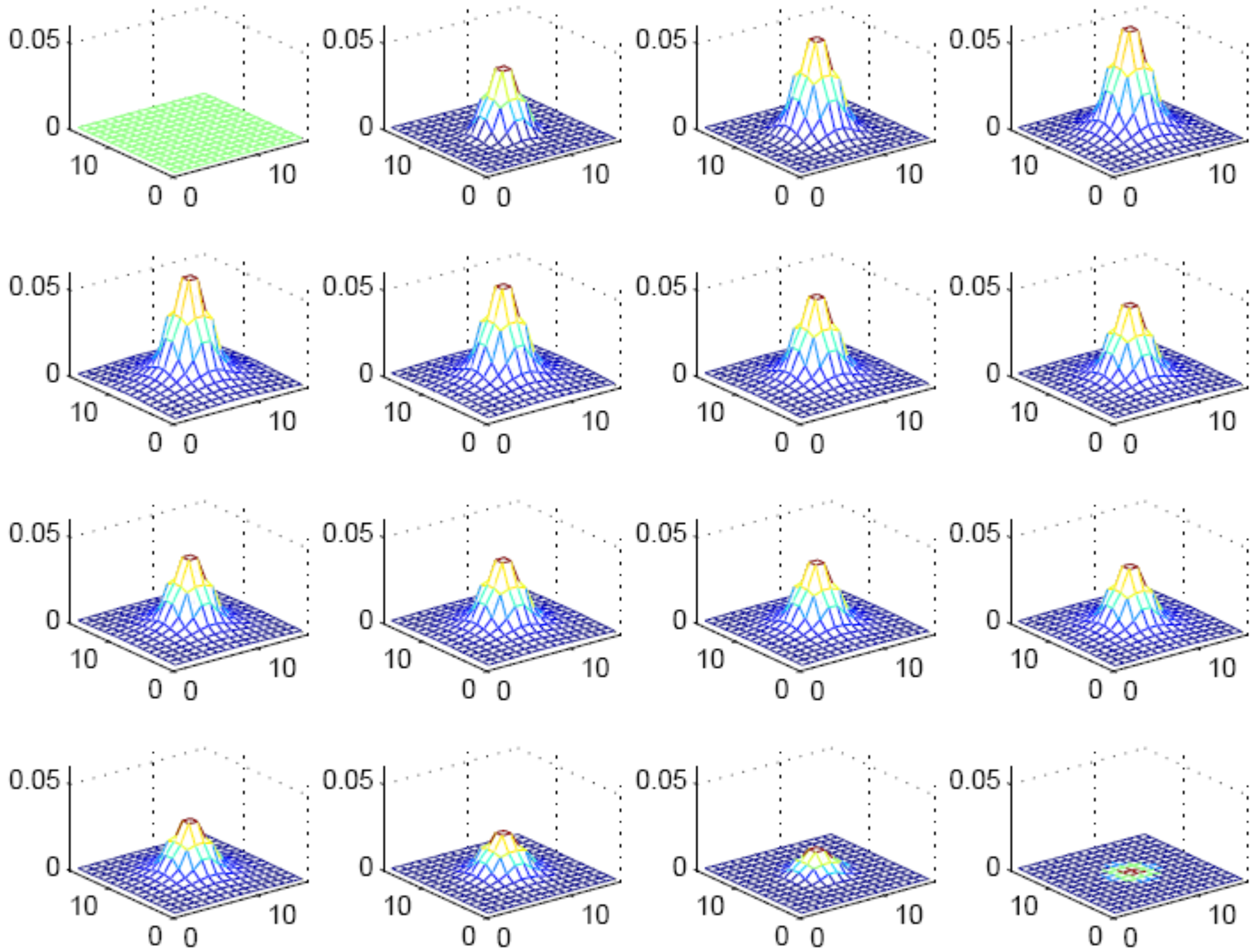

Series of images parameterized by the angle of Compton scattering ω $(5^0 < \omega < 175^0)$

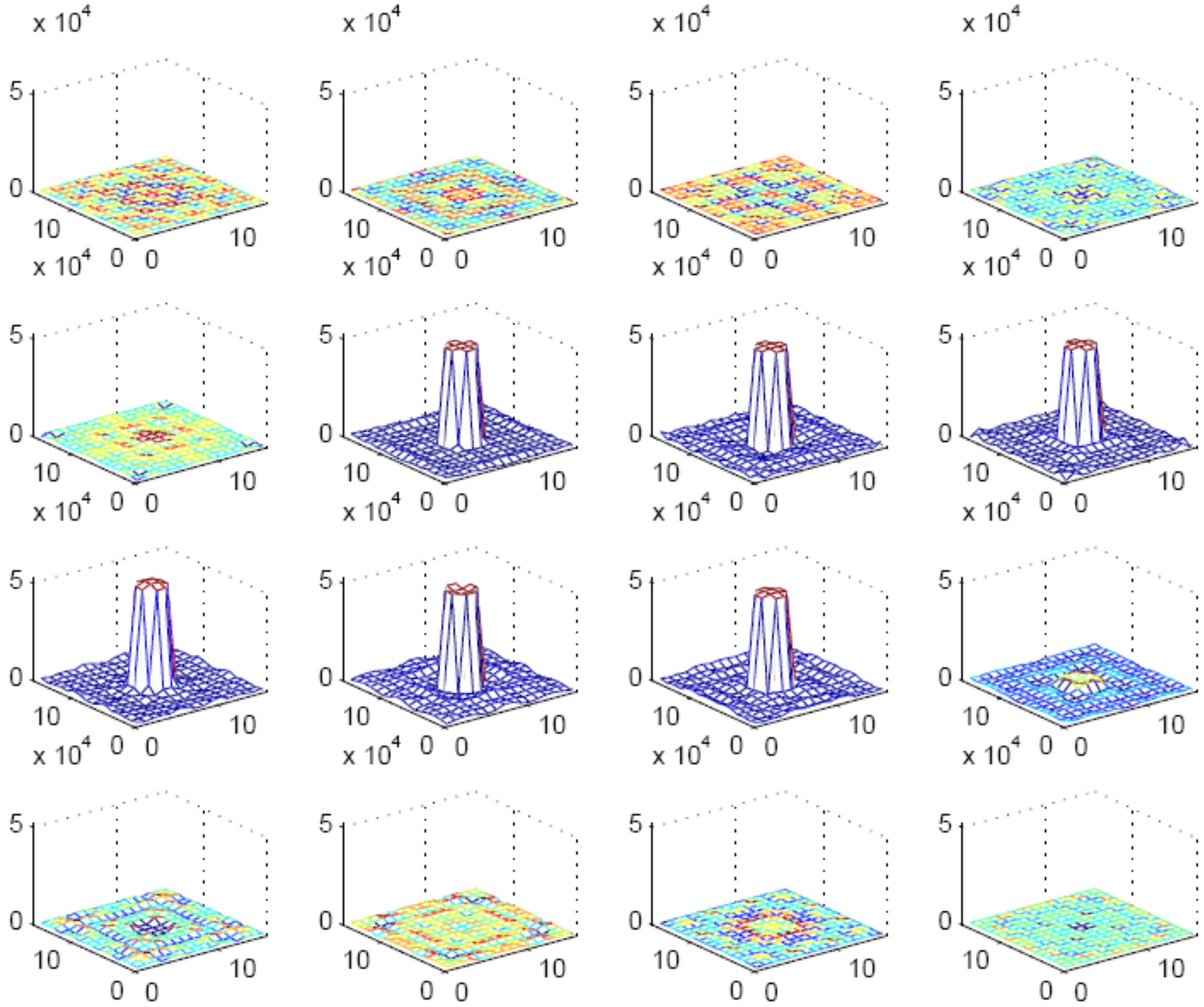

Reconstructed object in the absence of noise (RMSE = 1.2%)

(Nguyen M K, Truong T T, Driol C, Zaidi H, TNS - 2009)

2D Scattered Radiation Emission Imaging

the cone is now a V-line

Compounded V-Line projection.

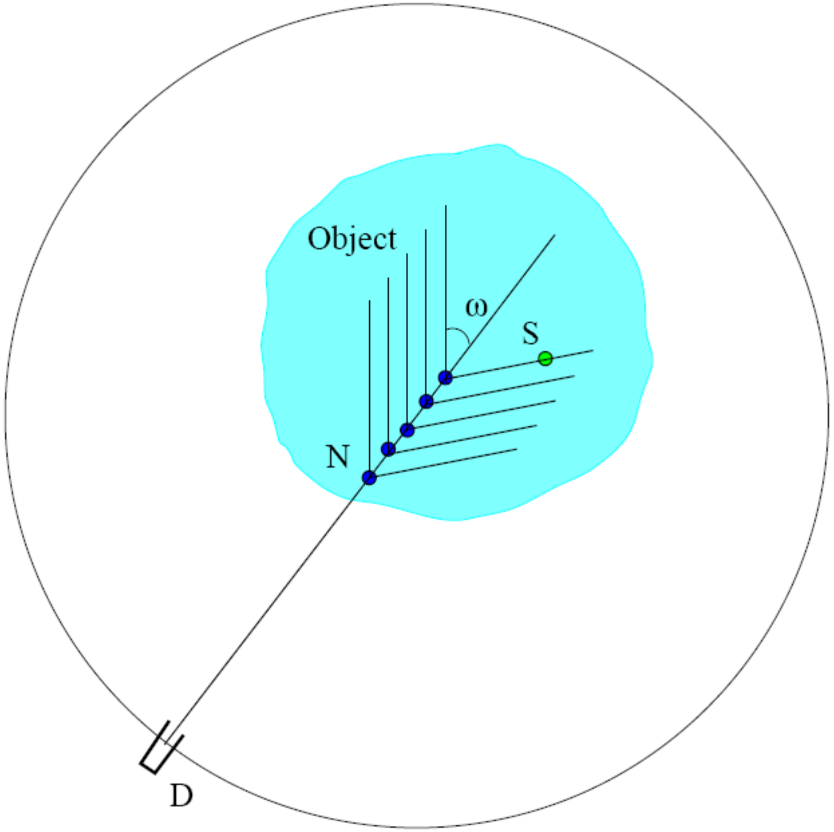

Collimated detecting pixel → Linear gamma camera

Image formation modeling:

Compounded V-Line Radon Transform (CVLRT) of $f(x,y)$

$$\widehat{f}(\zeta,\tau) = K^*(\tau)\int_0^\infty \frac{d\eta}{\eta}\int_0^\infty \frac{dr}{r}\,[f(\zeta + r\sin\omega, \eta + r\cos\omega) + f(\zeta - r\sin\omega, \eta + r\cos\omega)]$$

where

- $\tau = \tan\omega$,
- $K^*(\omega) = \pi r_e^2 n_e^* \mathcal{P}(\omega)$ (Klein-Nishina)
- $1/\eta$ and $1/r$ (Photometric factors in 2D)

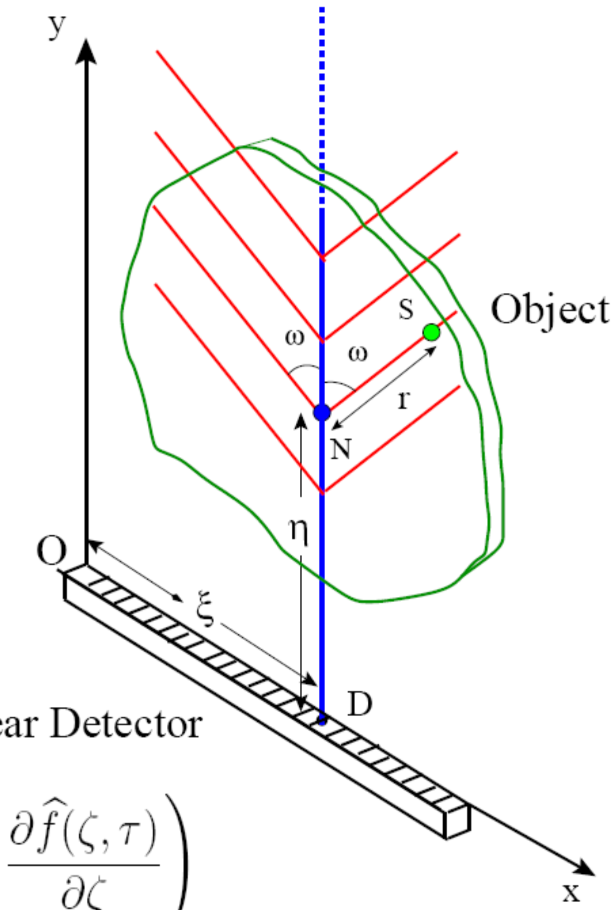

Inversion formula

$$f(x,y) = \int_{\mathbb{R}} dq\, e^{2i\pi qy}\,\frac{\int_{\mathbb{R}} dz\, e^{-2i\pi zq}\, h(x,z)}{(-)\left[\log 2\pi|q| + \gamma - i\frac{\pi}{2}\,\mathrm{sgn}q\right]}$$

under the same conditions as in 3D with

$$h(x,y) = \frac{y}{\pi}\int_0^\pi d\tau\left(\mathrm{P.V.}\int_{\mathbb{R}} d\zeta\left(\frac{1}{\zeta - x - y\tau} + \frac{1}{\zeta - x + y\tau}\right)\frac{\partial\widehat{f}(\zeta,\tau)}{\partial\zeta}\right)$$

2D Reconstruction

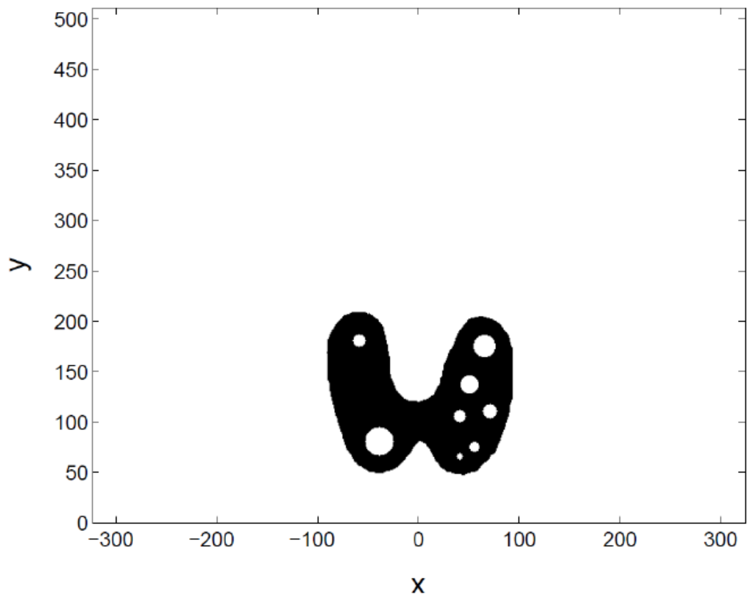

Original Thyroid phantom

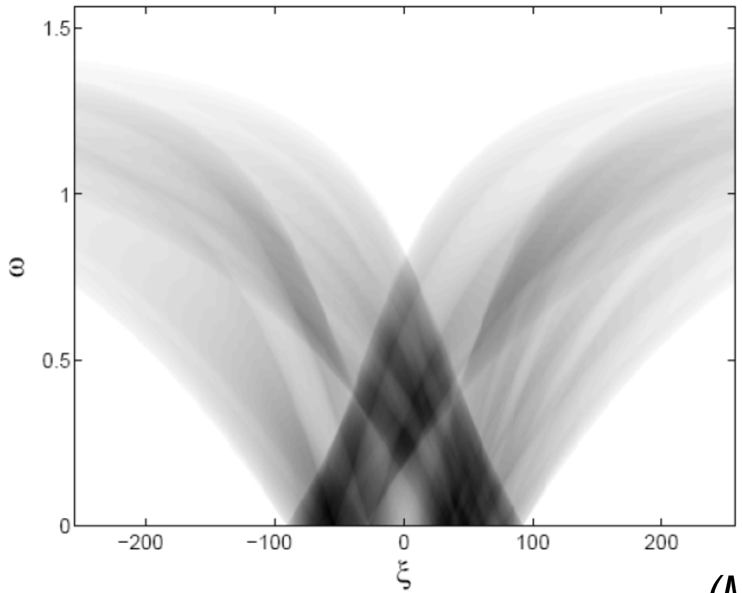

V-line data of the Thyroid

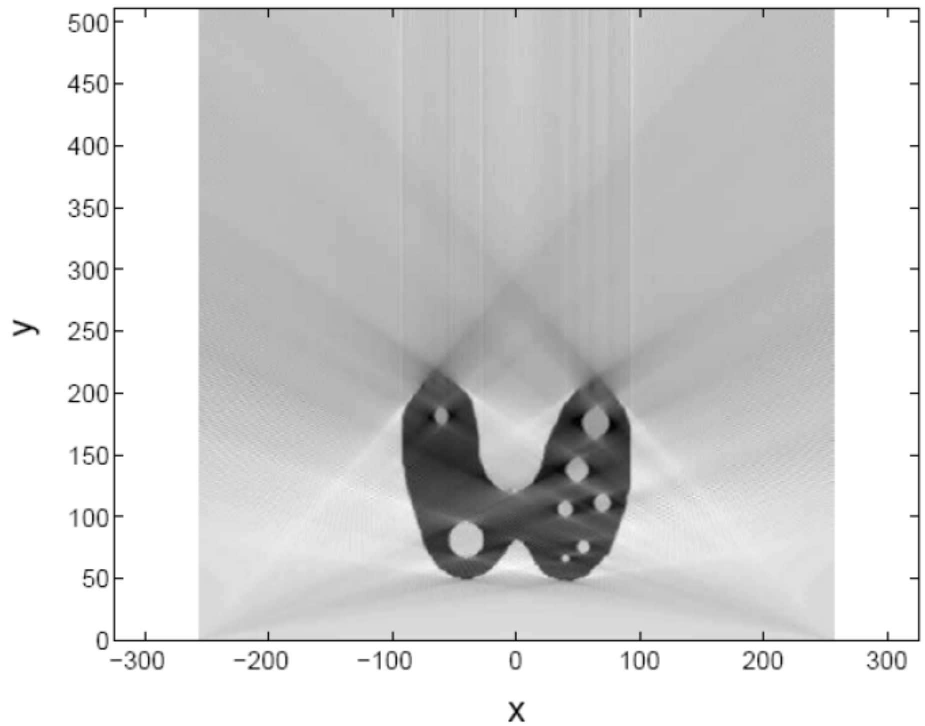

Reconstruction of
Thyroid phantom

(Morvidone M, Nguyen M K, Truong T T, Zaidi H, IJBI -2010)

B)Transmission-Scattering Tomographic Imaging

▪ Working conditions:
- Object is illuminated by external source S of known characteristics
- Detection of scattered photons by point-like detector D without collimator
- Collected photon flux density at D for given scattering angle ω comes from all scattering sites M on circular arcs subtending an inscribed angle of (π-ω).

➢ Because of the geometry of Compton scattering, this photon flux density is proportional to the integral of the object electron density $n(r,\theta)$ on such circular arcs

➢ Such integrals depend on two variables: ω the scattering angle and Φ the geometric position of the circular arc as measured from a reference direction.

➢ Up to now, two possible ways to vary the relative positions of the source S and the detector D in the plane lead to two working modalities for Compton Scatter Tomography (CST):

Norton (1995) and a new modality (2010)

1) Norton's modality (1995)

- Source S at fixed position
- Detector D moving along an axis passing through S
- Object is situated on one side of the axis SD
- Radiation spreading and attenuation not accounted for

➢ Modeling by Radon transform on circles intersecting a fixed point with equation

$$r = p\cos(\theta - \phi)$$

$\hat{n}(p,\phi)$: transform of the electron density $n(r,\theta)$

$$\hat{n}(p,\phi) = \int_{\mathrm{arc}\,SD} ds\; n(r, \gamma + \phi)$$

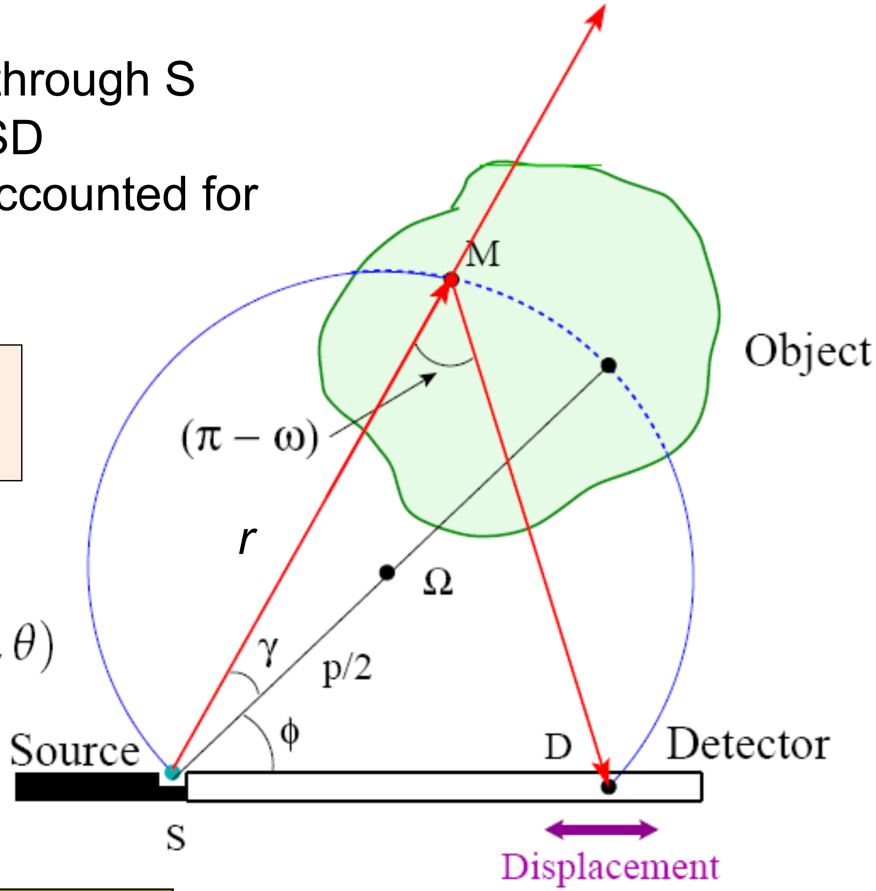

➢ Analytic Inversion Formula (Cormack (1964))

$$n(r,\theta) = \frac{1}{2\pi^2 r}\int_0^{2\pi} d\phi \int_0^{\infty} dp\, \frac{\partial \hat{n}(p,\phi)}{\partial p}\,\frac{1}{r/p - \cos(\theta - \phi)}$$

Simulation results on Radon transform on circles through O

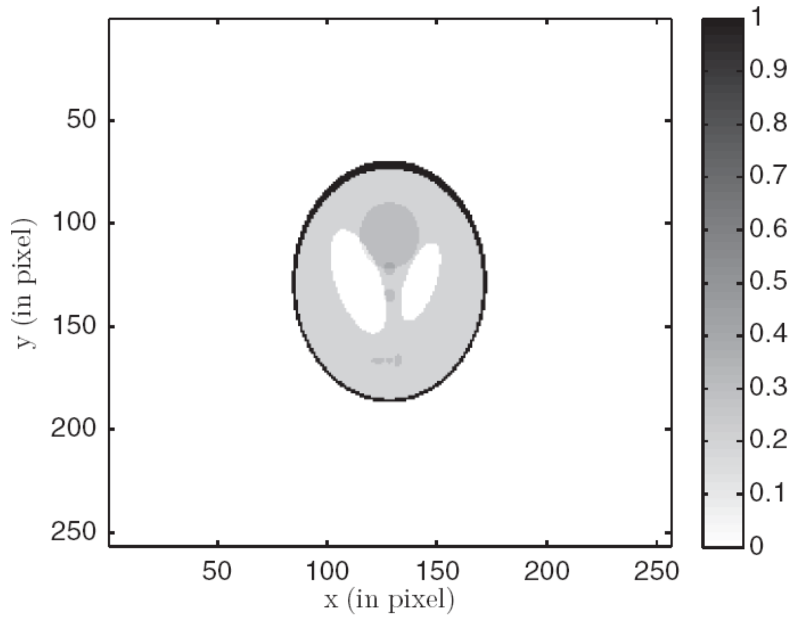

Original Shepp-Logan phantom

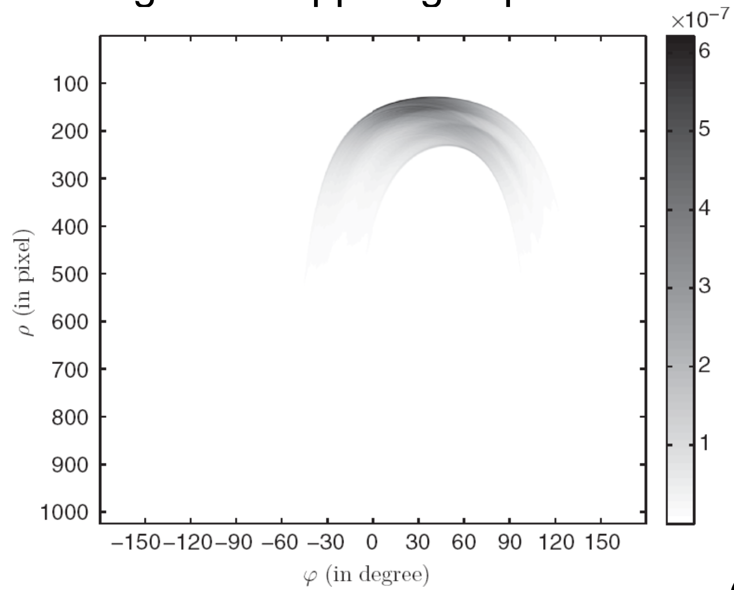

Radon data of the SL phantom

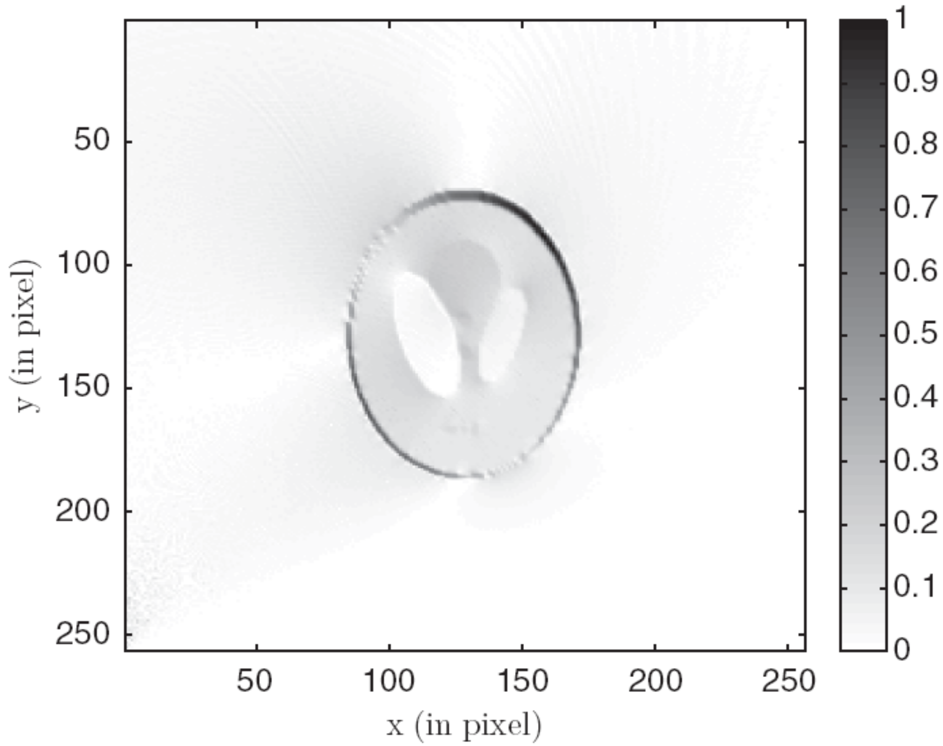

Reconstructed SL phantom with

NMAE = 3.6% and NMSE = 0.5%

(G. Rigaud, M. K. Nguyen and A. K. Louis, IPSE - 2012)

2) Our modality (Inverse Problems 2010)

- Object inside circle (Γ_p) centered at O and of radius *p*
- Source S and Detector D on a rotating diameter of (Γ_p)
- Radiation spreading and attenuation not accounted for

➢ Radon transform on circular arcs subtended by a rotating chord of fixed length: integration of a function *f* on circular arc of equation

$$r = r(\cos\gamma) = p\left(\sqrt{1+\tau^2\cos^2\gamma} - \tau\cos\gamma\right)$$

$\widehat{n}(p,\phi)$, the transform of $n(r,\theta)$ is

$$\widehat{n}(p,\phi) = \int_{\mathrm{arc}\,SD} ds\; n(r,\gamma+\phi)$$

where *ds* is the arc measure and

$\theta = (\varphi - \gamma)$, τ = *cotan* ω

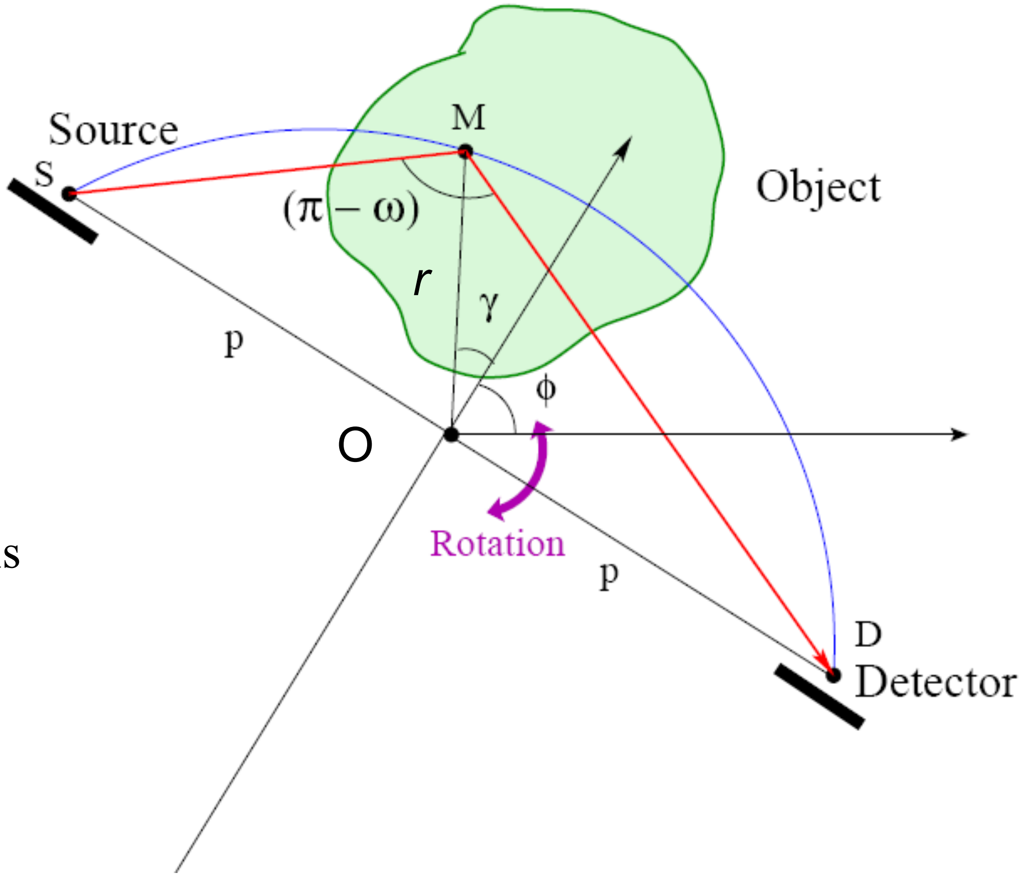

Inversion *via* mapping back to the Radon transform on circles intersecting the origin O and using this inversion procedure with

• new variable

$$g = \frac{1}{2}\left(\frac{p}{r} - \frac{r}{p}\right)$$

• new function

$$N(g,\theta) = \frac{\tau \;\; n(r,\theta)}{\sqrt{1+\tau^2}}$$

• Analytic inversion formula

$$n(r,\theta) = \frac{1}{2\pi^2} \frac{\sqrt{1+\frac{1}{4}\left(\frac{p}{r}-\frac{r}{p}\right)^2}}{\frac{r}{2}\left(\frac{p}{r}-\frac{r}{p}\right)} \int_0^{2\pi} d\phi \int_0^{\infty} d\tau \, \frac{1}{\frac{1}{2\tau}\left(\frac{p}{r}-\frac{r}{p}\right) - \cos(\theta-\phi)} \frac{\partial}{\partial\tau}\left(\frac{\tau\, \hat{n}(\tau,\phi)}{\sqrt{1+\tau^2}}\right)$$

Simulation results for the NT's modality

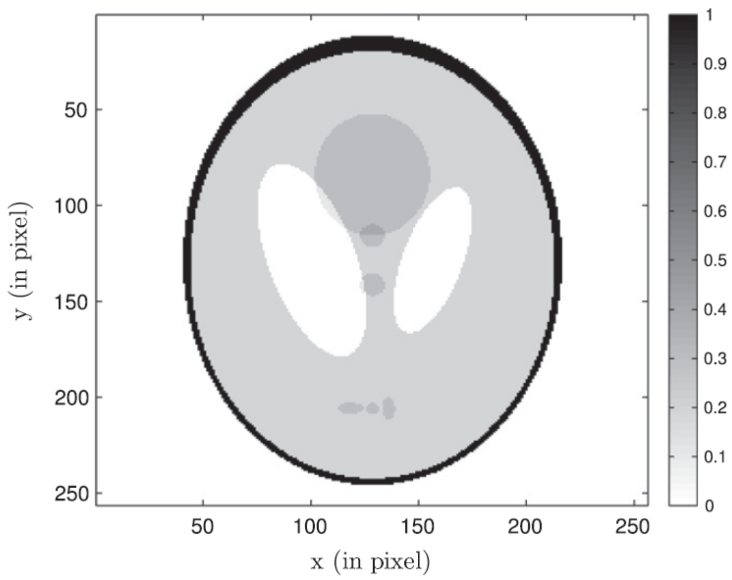

Original Shepp-Logan (SL) phantom

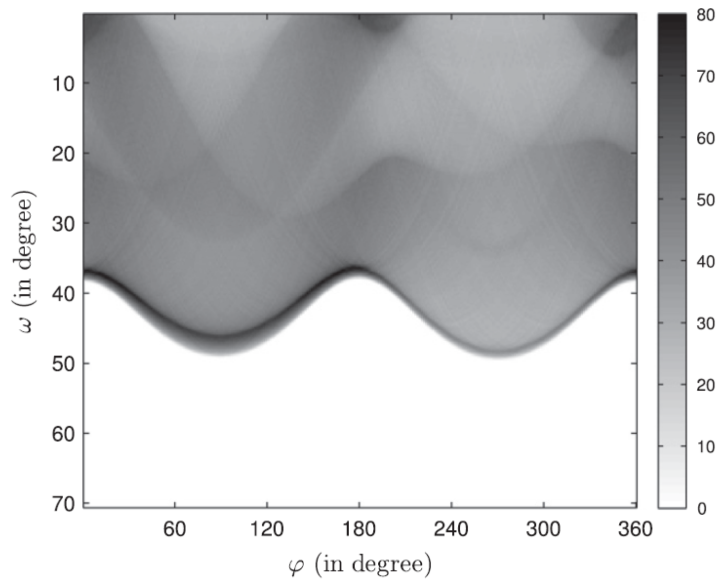

Projection data in NT's modality

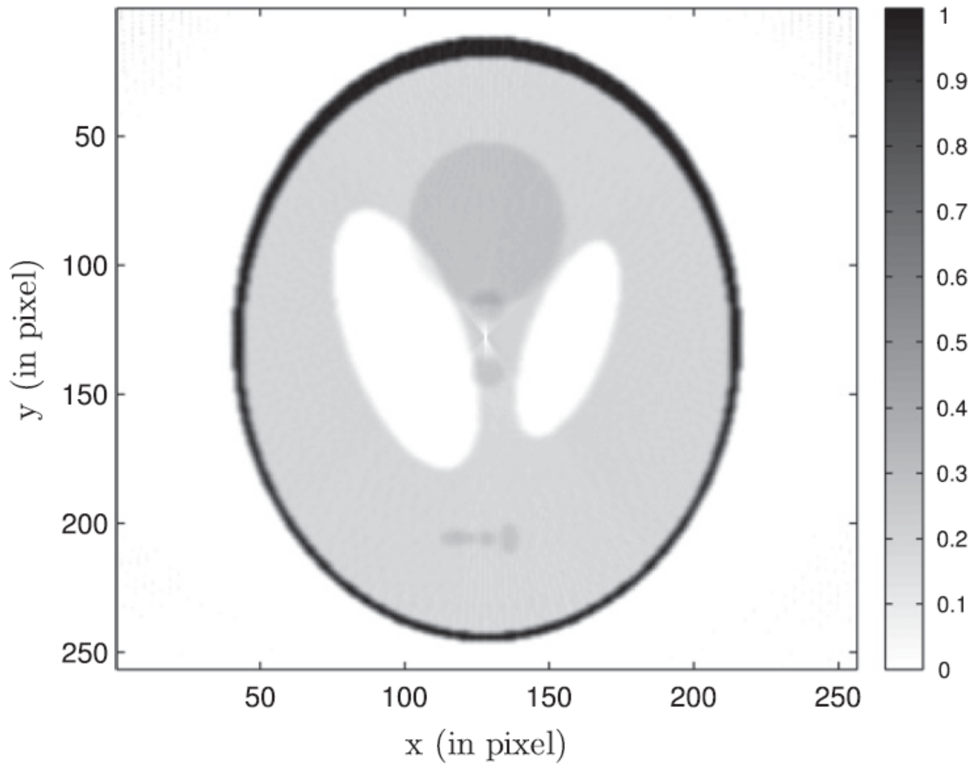

Reconstructed SL phantom in NT's modality

(*G. Rigaud, M. K. Nguyen and A. K. Louis, IPSE - 2013*)

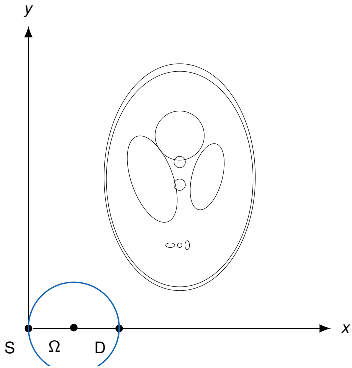
y
x
S
Ω
D

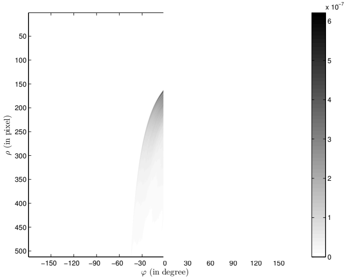
ρ (in pixel)
φ (in degree)
50
100
150
200
250
300
350
400
450
500
−150 −120 −90 −60 −30 0 30 60 90 120 150
x 10^−7
0 1 2 3 4 5 6

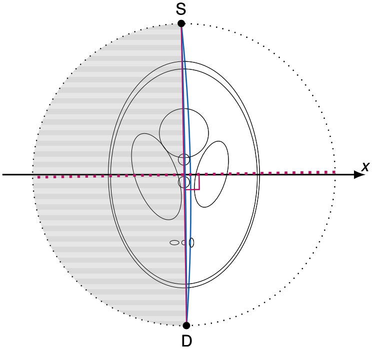
S
x
D

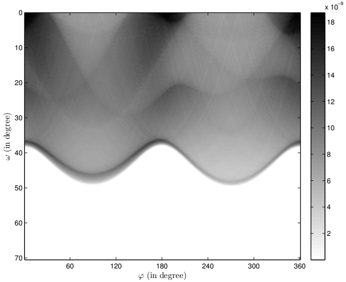
x 10^-9
ω (in degree)
φ (in degree)
0
10
20
30
40
50
60
70
60
120
180
240
300
360
18
16
14
12
10
8
6
4
2

3) Bimodal Compton Scatter radiation imaging (2013)

Combining two modalities of scattered radiation imaging

1) Norton's Compton scatter tomography CST_1
2) 2D scattered radiation emission tomography CST_2

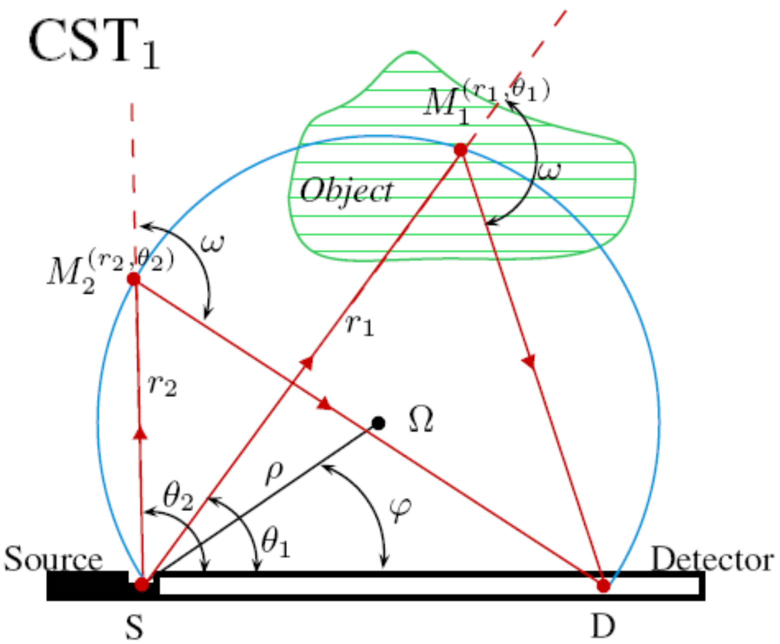

Principle of Norton's modality of Compton scattering tomography

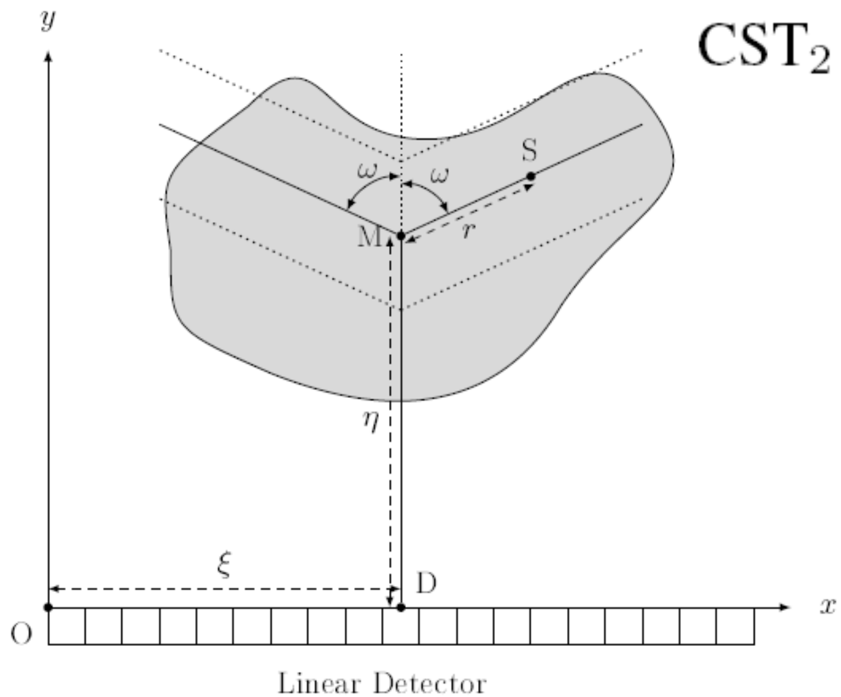

Principle of compounded $\mathcal{V}$-line Radon transform

Treatment of attenuation

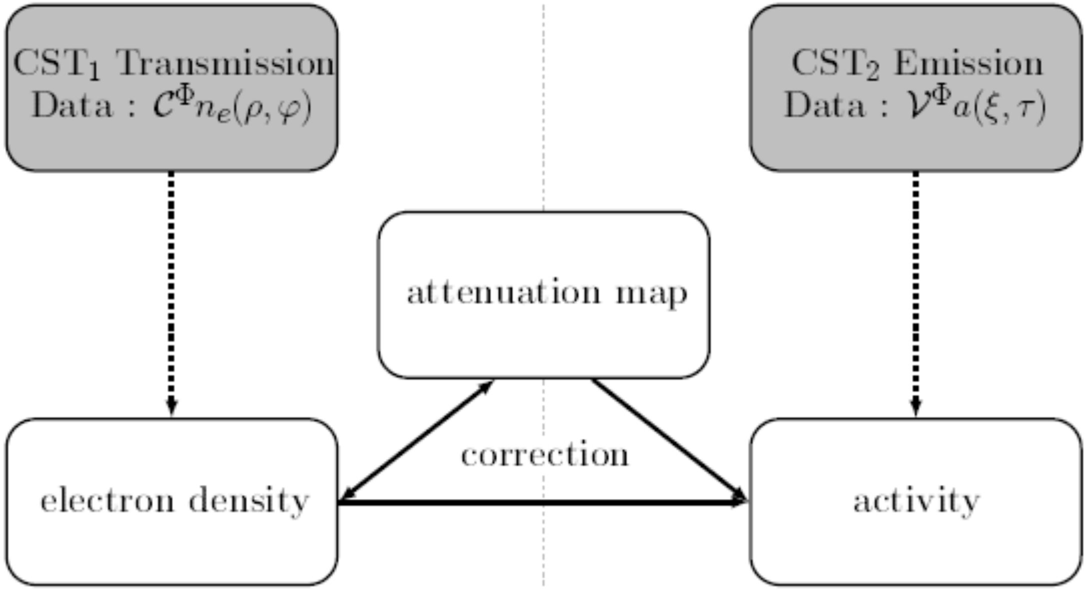

Concept of a novel bimodal system

- Image formation with attenuation factor

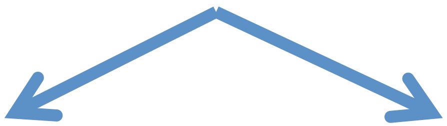

- Inversion of $\mathcal{C}$ without attenuation factor
- Inversion of $\mathcal{V}$ without attenuation factor

Attenuation correction

$$F^{n+1} = F^n + D_m^{-1} T^{-1} \circ (G - T^{\phi} F^n)$$

with

- $F^0 \equiv 0$
- $T \equiv \mathcal{C}$ or $\mathcal{V}$
- $G = \mathcal{C}^{\Phi} n_e$ or $\mathcal{V}^{\Phi} a$
- $D_m =$ maximum of the distorsion kernel

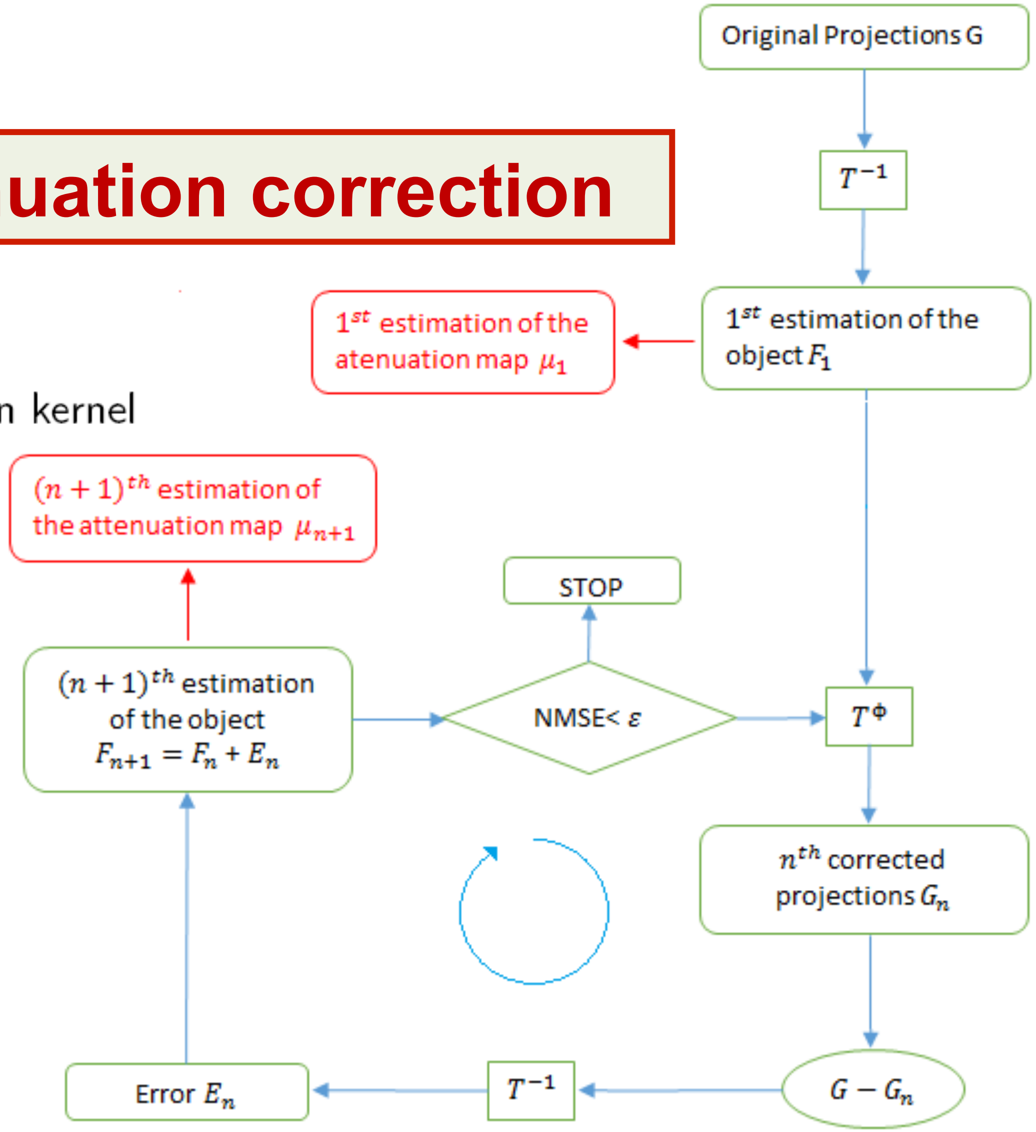

- *Prior information : we know the kind of matters inside the studied object.*
- *K-means is performed to estimate attenuation map at each step from the estimate of the electron density.*

Simulation Results

Zubal phantom

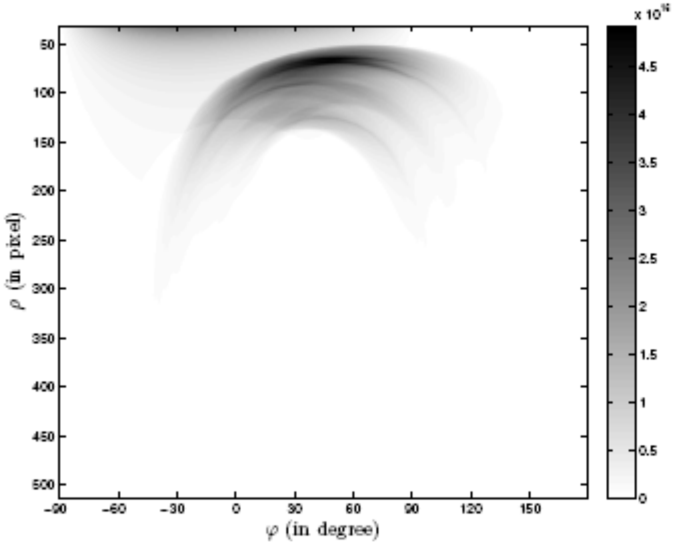

CST_1

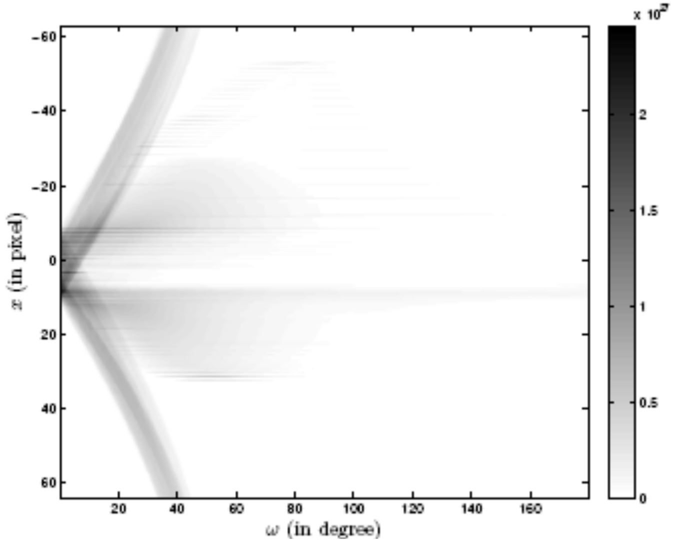

CST_2

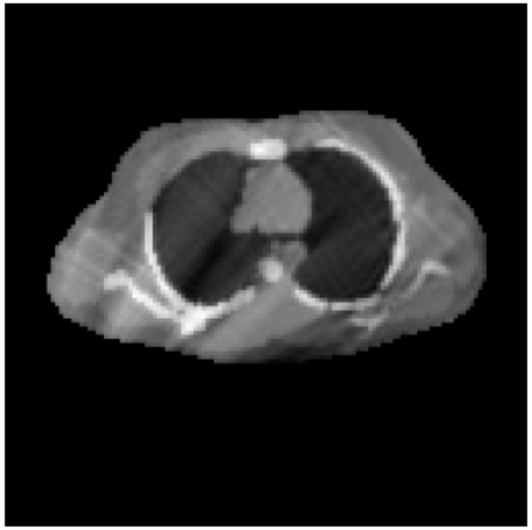

electron density

activity distribution

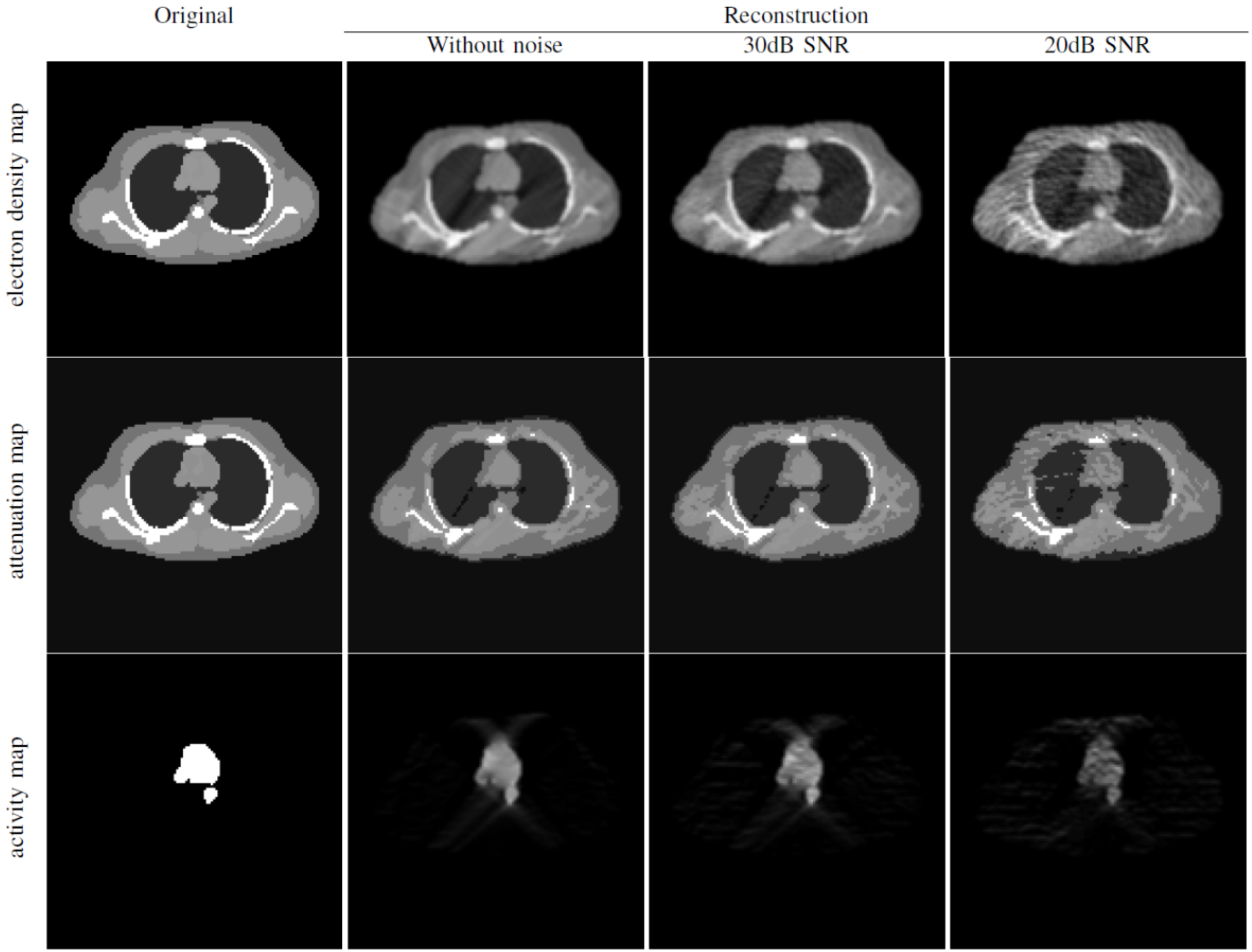

Different reconstructions of the electron density map, attenuation map for different SNR

NMSE of n_e

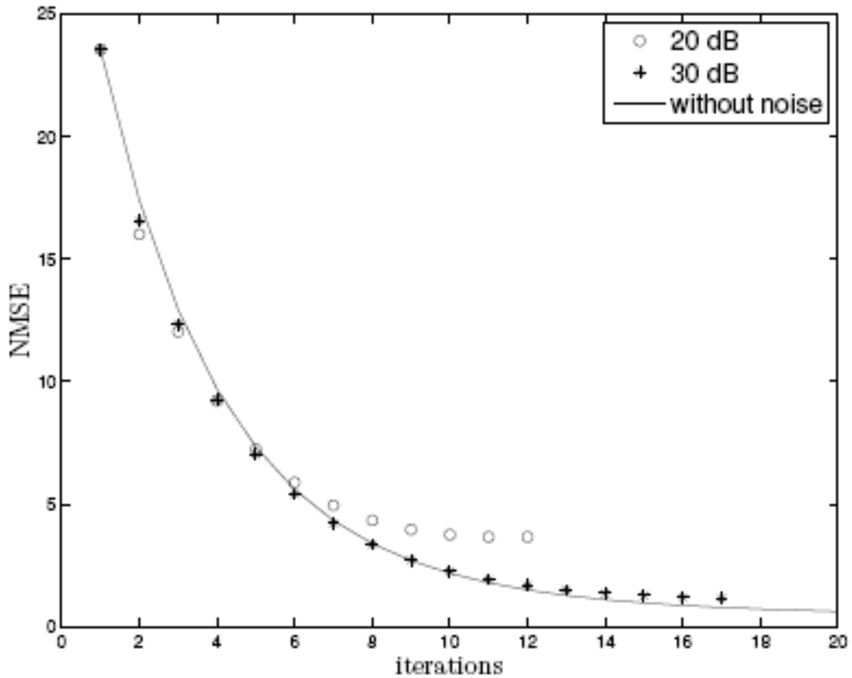

NMSE of a

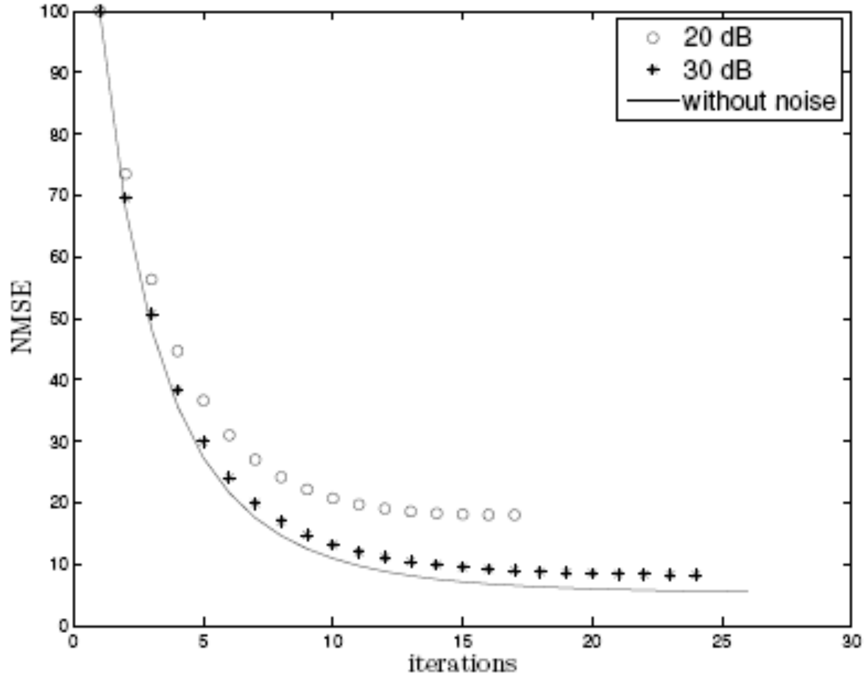

Conclusions

Applications

- Non-destructive testing
- Biomedical imaging

Advantages

- Estimation of n_e, μ and a
- Reconstruction without rotation
- Efficient and generalized correction algorithm

CONCLUSION

• **New imaging concepts exploiting scattered radiatio**

•**New imaging modalities (emission, transmission, bimodality)**

• **Mathematical modelling by generalized Radon Transforms (RT)**
(V-line, Conical, circular arcs RT)

Advantage: New operating scheme without detector rotation (planar detector in 3D and linear detector in 2D) in emission imaging for activity reconstruction

Advantage: New tomographies using point source – point detector in relative motion on a curve (line or circle) for direct electron density reconstruction

4) Bibliography (1)

-G Rigaud, R Régnier, M K Nguyen, 2013
Combined modalities of Compton scattering tomography
IEEE Trans. Nucl. Sci. (to appear)

- G. Rigaud, M. K. Nguyen and A. K. Louis, 2012
Novel numerical inversions of two circular-arc Radon transforms in Compton scattering tomography,
***Inverse Problems in Science and Engineering* 20(6):809-839.**

- G. Rigaud, M. K. Nguyen and A. K. Louis, 2013
Modelling and simulation results on a new Compton scattering tomography
***Simulation Modelling Practice and Theory,* 33 :28-44.**

- Truong T T , Nguyen M K , 2011
Radon transforms on generalized Cormack's curves and a new Compton scatter tomography modality,
***Inverse Problems* 27 : 125001**

- Truong T T, Nguyen M K, 2011
On new V-line Radon transforms in R^2 and their inversion,
***J. Phys. A: Math. Theor.* 44, 075206**

4) Bibliography (2)

- **Nguyen M K, Truong T T, 2010**
  Inversion of a new circular-arc Radon transform for Compton tomography,
  ***Inverse Problems* 26 (6): 065005 (Highlights IP 2010)**

- **Morvidone M, Nguyen M K, Truong T T, Zaidi H, 2010**
  A novel V-line Radon transform and its imaging applications*,*
  International Journal of Biomedical Imaging,
  Special issue on Mathematical Methods for Images and Surfaces,
  Vol. 2010, Article ID 208179, 6 pages, DOI:10.1155/2010/208179

- **Nguyen M K, Truong T T, Driol C, Zaidi H, 2009**
  On a novel approach to Compton scattered emission imaging
  ***IEEE Trans. Nuclear Science* 56(3): 1430-1437**

- **Nguyen M K, Truong T T, 2002**
  On an Integral Transform and its Inverse in Nuclear Imaging
  ***Inverse Problems* 18: 265-277**

Thank you for your attention